Noise Analysis of the Glutamate-Activated Current in Photoreceptors

H. P. Larsson, S. A. Picaud, F. S. Werblin, and H. Lecar
Division of Neurobiology, Department of Molecular and Cell Biology, University of California, Berkeley, California 94720 USA

ABSTRACT The glutamate-activated current in photoreceptors has been attributed both to a sodium/glutamate transporter and to a glutamate-activated chloride channel. We have further studied the glutamate-activated current in single, isolated photoreceptors from the tiger salamander using noise analysis on whole-cell patch-clamp recordings. In cones, the current is generated by chloride channels with a single-channel conductance of 0.7 pS and an open lifetime of 2.4 ms. The number of channels per cell is in the range of 10,000- 20,000. Activation of the channels requires the presence of both glutamate and sodium. The single-channel conductance and the open lifetime of the channel are independent of the external concentration of glutamate and sodium. External glutamate and sodium affect only the opening rate of the channels. D,L-Threo-3-hydroxyaspartate (THA), a glutamate-transport blocker, is shown to be a partial agonist for the channel. The single-channel conductance is the same regardless of whether glutamate or THA is the ligand, but the open lifetime of the channel is only 0.8 ms with THA as ligand. The glutamate-activated current in rods has a similar single-channel conductance (0.74 pS) and open lifetime (3 ms). We propose a kinetic model, consistent with these results, to explain how a transporter can simultaneously act both as a sodium/glutamate-gated chloride channel and a glutamate/sodium cotransporter.

INTRODUCTION

In cones, glutamate was reported to gate a chloride channel (Sarantis et al., 1988; Tachibana and Kaneko, 1988; Everett et al., 1990; Picaud et al., 1995a). The current was attributed to a glutamate-activated chloride channel because the reversal potential of the current closely follows the Nernst potential of chloride (Sarantis et al., 1988; Picaud et al., 1995a) and because increased chloride current is accompanied by a measurable increase in current noise (Tachibana and Kaneko, 1988; Everett et al., 1990; Picaud et al., 1995a).

Surprisingly, this glutamate-activated channel also exhibits some phenomenogical features that are usually attributed to glutamate transporters. For example, agonists of classical glutamate receptors do not activate the channel, whereas the usual glutamate transport substrates elicit a current. Similarly, antagonists of classical glutamate receptors have no effect on the glutamate-elicited current, whereas glutamate-transport blockers suppress the current (Grant et al., 1992; Grant, 1992; Eliasof and Werblin, 1993). As with sodium-dependent transporters, external sodium is required to elicit a current, and lithium cannot substitute for external sodium in generating the current (Sarantis et al., 1988; Tachibana and Kaneko, 1988).

Because of the sodium dependence and the pharmacology of the current, earlier investigators hypothesized that a sodium/glutamate transporter was involved in generating the current (Tachibana and Kaneko, 1988; Eliasof and Werblin, 1993). It had also been shown earlier that radioactively labeled glutamate is taken up into photoreceptors (Marc and Lam, 1981). In an earlier work, the similarities (in ionic dependencies and pharmacology) between the glutamate transporters and the glutamate-activated chloride channel led us to suggest that glutamate transport may gate the chloride channel (Picaud et al., 1995a).

In this paper, we further analyze the properties of the glutamate-gated chloride channel to determine whether this channel is a conventional ligand-gated channel despite its sodium dependence and unusual pharmacology. As the conductance of the glutamate-gated chloride channel is too small for single channel recording, it was investigated by using noise analysis of the current. Furthermore, we investigated whether the glutamate-elicited current in rods is generated by a similar channel.

MATERIALS AND METHODS

Cell dissociation

Single isolated photoreceptors from tiger salamanders were mechanically dissociated as described earlier (Eliasof and Werblin, 1993). The retina was cut into square pieces about 100 μm on a side and kept in Ringer's solution at 4°C. The cells were dispersed in the recording chamber with a fire-polished Pasteur pipette just before a recording session.

Whole-cell current recording

Single isolated photoreceptors were recorded in the whole-cell configuration of the patch-clamp technique (Hammill et al., 1981). The cells were continuously perfused with Ringer's solution (1 ml/min) through a gravity-feed perfusion system. The Ringer's solution contained 108 mM NaCl, 1 mM $MgCl_2$, 1 mM $CaCl_2$, 5 mM HEPES, 2.5 mM KCl, and 3 mM glucose and was titrated to pH 7.8 with NaOH. Recordings were made in a solution containing 100.5 mM NaCl, 1 mM $MgCl_2$, 1 mM $BaCl_2$, 0.1 mM $CoCl_2$, 5 mM HEPES, 10 mM TEA-Cl, and 3 mM glucose and titrated to pH 7.8 with NaOH. Drugs were added to this recording solution without substitution and applied through bath application. Free glutamate concentrations have been calculated using critical stability constants (Martell and Smith,

Received for publication 31 July 1995 and in final form 2 November 1995.
Address reprint requests to Dr. Harold Lecar, MCB, Stanley/Donner ASU, University of California, Berkeley, CA 94720. Tel.: 510-643-8875; Fax: 510-643-9290.

0006-3495/96/02/733/00 $2.00

1974) and the Maxchelator software program (Chris Patton, Pacific Grove, CA).

Pipettes were made from thick-walled borosilicate glass capillaries (SE16; Dagan Co., Minneapolis, MN) and pulled with a Sachs-Flaming puller. The pipettes were filled with a solution containing 119 mM KCl, 1 mM MgCl, 0.1 mM CaCl, 0.1 mM BaCl, 1.27 mM BAPTA, 4 mM HEPES, 5 mM NaATP, and 0.1 mM NaGTP. Solutions were titrated to pH 7.4 with KOH. The pipettes had a resistance of 2–3 MΩ, and the series resistance in the whole-cell mode was usually in the 5–10 MΩ range.

Whole-cell voltage and currents are controlled and amplified by a LIST L/M EPC-7 patch-clamp amplifier. The amplified currents were filtered through an eight-pole Bessel filter and fed through a TL-1 Interface (Axon Instruments, Foster City, CA) to an IBM-AT computer. The current signal was continuously recorded on a hard disk using an AxoTape program (Axon Instruments).

Noise analysis of whole-cell currents

The noise analysis was carried out on AxoTape files using the CAP program (RC-electronics). Measurements of the variance and the mean currents were made on slow washouts of agonists at constant voltage. The variance and the mean were calculated on subrecords of 500 ms filtered at 500 Hz or 1000 Hz. This gives a bandwidth of 2–500 Hz (or 2–1000 Hz). The length of the subrecords (500 ms) was chosen so that the decline of current during the washout would introduce only a small error in the variance measurements (<0.5 pA^2) and that not too much of the variance from the low frequencies would be cut out (<2%). The upper limit of the bandwidth, set by the external filter, was chosen so that the corner frequency of the expected spectrum was approximately one-fifth of the upper frequency of the bandwidth. The frequencies that are cut off give an error of less than 10% for the variance.

Power spectra are calculated and averaged from long records (30–90 s) at constant agonist concentration and membrane voltage. Fast-Fourier transforms were made on subrecords of 2048 points filtered at either 500 Hz or 1000 Hz. This gives a bandwidth of 0.5–500 Hz for the records filtered at 500 Hz and acquired at 1 kHz. For the records filtered at 1 kHz and acquired at 2 kHz the bandwidth is 1–1000 Hz. The spectra shown are the result of averaging 30–60 spectra from the same cell.

The maximal bandwidth of the recordings was limited by the RC product of the cell membrane capacitance and the pipette resistance. The filter frequency of the external filter was always set below this maximal bandwidth of the recording. Recordings in this work have a bandwidth of 0–1000 Hz (and in some cases only up to 500 Hz).

Results are given as mean ± SD (number of cells).

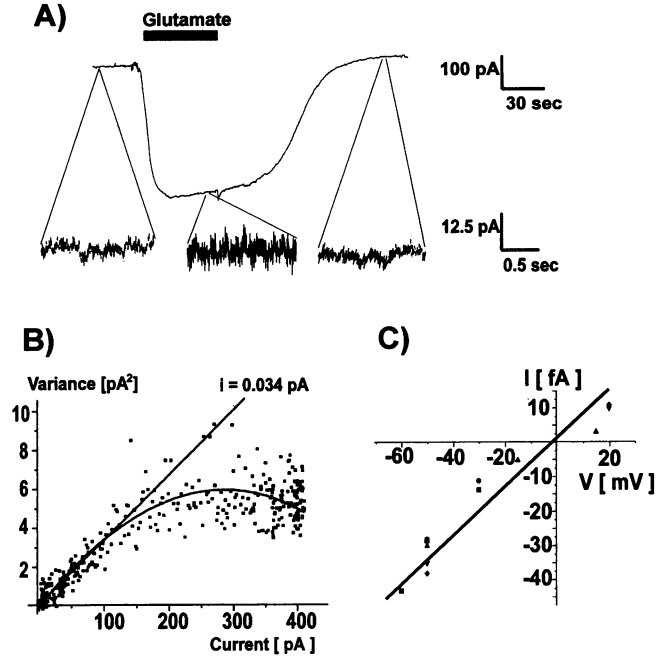

FIGURE 1 Noise analysis of the glutamate-gated current fluctuations. (*A*) A whole-cell recording from a cone photoreceptor held at −50 mV during a bath application of 1 mM glutamate. Enlarged sections of the record shown are from before, during, and after glutamate application. The increase of current was accompanied by a visible increase in noise. The signal is filtered at 1000 Hz. (*B*) Variance-versus-mean plot of the current from the washout of 1 mM glutamate. The data are fitted to the equation $\mathrm{Var}(I) = iI - I^2/N$. The straight line is the asymptote at 0 glutamate and has a slope of 0.034 pA. This corresponds to a single-channel conductance of 0.68 pS at a holding potential of −50 mV. N was found to be 19,000. The maximum open probability is 0.65. (*C*) The single-channel current estimates from variance-versus-mean curves recorded in symmetrical chloride concentrations for voltages between −60 mV and +20 mV for five different cells. For each cell the single-channel current was measured first at −50 mV and then the experiment was repeated at a different voltage. Measurements from the same cell are marked with the same symbol. The best linear fit has a slope of 0.7 pS and goes through −2 mV.

RESULTS

Single isolated photoreceptors from the tiger salamander were recorded under voltage clamp at a holding potential of −50 mV. Glutamate elicits an inward current as shown in Fig. 1 *A* for a cone and in Fig. 2 *A* for a rod. The glutamate-elicited current is accompanied by a visible increase in the peak-to-peak noise of the current trace (Fig. 1 *A* and Fig. 2 *A*). This increase in current fluctuations indicates that glutamate gates a channel in both photoreceptor types.

Variance-versus-mean current plot gives single-channel conductance and number of channels per cell

When glutamate concentrations are varied from 0 glutamate up to saturating glutamate concentration (1 mM), the variance-versus-mean curve is best fit to a parabola (Fig. 1 *B*). The parabola further demonstrates that the glutamate-elicited current (I) is going through ionic channels with a stochastic gating process. For N independent channels with a single channel current (i) and an open probability (p), the average macroscopic current I and the variance of the current are defined in Eqs. 1 and 2, respectively:

$$I = Npi \tag{1}$$

$$\mathrm{Var}(I) = \mathrm{Ni}^2p(1 - p). \tag{2}$$

Substituting for p from Eq. 1 into Eq. 2 leads to a parabolic relation for the variance versus mean:

$$\mathrm{Var}(I) = Ii - I^2/N. \tag{3}$$

The number of channels (N) and the single channel current (i) are found by a least-square fit of the variance-versus-mean curve to Eq. 3. The single-channel current (i), at a holding potential of −50 mV, is 0.035 pA ± 0.004 pA (n = 5) in

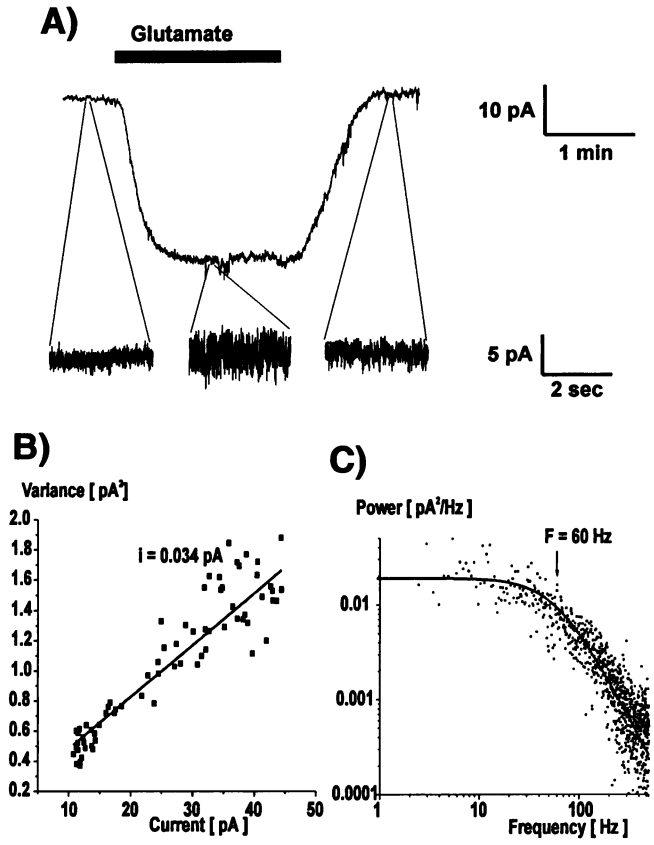

FIGURE 2 Characteristics of the glutamate gated channel in rods. (*A*) A whole-cell recording from a rod photoreceptor held at −50 mV during a bath application of 37 μM free glutamate. The increase of current was accompanied by a visible increase in noise. The signal is filtered at 500 Hz. (*B*) Variance-versus-mean plot of the current from the washout of 37 μM free glutamate. The data are fitted to a straight line and have a slope of 0.034 pA. This corresponds to a single-channel conductance of 0.68 pS at a holding potential of −50 mV. (*C*) Power spectrum during a 37 μM free glutamate application. The background spectrum has been numerically subtracted. The corner frequency is 60 Hz.

symmetrical 100 mM chloride concentration. The single-channel current was found from the fit to the parabola or in some cases estimated from the slope of the variance-versus-mean curve at low open probabilities (see Channel Characteristics in Rods). The single-channel current can be measured by noise analysis at different holding potentials to obtain a single-channel current-voltage curve. In symmetrical chloride concentrations, the single-channel current-voltage curve is best fit with a straight line crossing the abscissa at −2 mV, which is close to the equilibrium potential for chloride (0 mV), and with a slope of 0.7 pS (Fig. 1 *C*). This result indicates that the glutamate-induced noise results from a channel with an estimated single-channel conductance of 0.7 pS. The number of channels in a cone cell was found to range from 10,000 to 20,000 channels/cell. The open probability at the maximum obtainable current (1 mM glutamate applied) is 0.7 ± 0.05 (n = 3).

The power spectra fit single Lorentzians

Power spectra were calculated in the absence (Fig. 3 *A*) and in the presence (Fig. 3 *B*) of glutamate. The power spectrum of the glutamate-elicited current was calculated by sustracting the fitted power spectrum obtained in the absence of glutamate to the power spectrum obtained in the presence of glutamate for the same cell. The power spectra of the glutamate-elicited current are best fit with a single Lorentzian at all concentrations of glutamate. At saturating concentration (1 mM), the power spectrum is best fit with a Lorentzian having a corner frequency of 220 Hz ± 10 Hz (n = 3) (Fig. 3 *C*). In a simple model of ligand activation where the binding of one glutamate opens the channel (see Discussion), the closing rate is independent of the glutamate concentration. By contrast, the opening rate is dependent on the glutamate concentration and therefore it is expected that the corner frequency would increase with increasing glutamate concentration. At a free glutamate concentration of 37 μM, which gives an open probability of 0.5, the corner frequency is decreased to 118 Hz ± 10 Hz (n = 6). At even lower glutamate concentration (6 μM), which gives an open

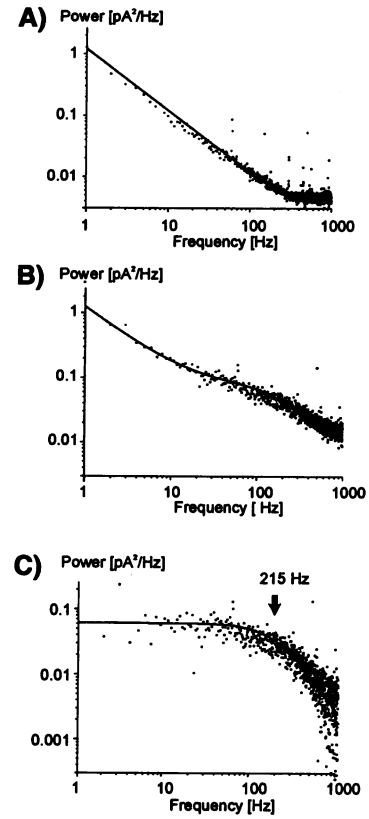

FIGURE 3 Corner frequency of the glutamate elicited current. Power spectra of whole-cell currents for a cone held at −50 mV. The spectrum is an average of 30 spectra, each calculated from a 2-s trace. (*A*) The background 1/*f* spectrum recorded at 0 glutamate. (*B*) The spectra measured when 1 mM glutamate was applied. (*C*) The spectra from *B* with the fitted background from *A* numerically subtracted. The corner frequency of the Lorentzian is 215 Hz.

probability of 0.2, the corner frequency is decreased to 80 ± 10 Hz (n = 5).

Channel characteristics in rods

Application of 37 μM glutamate onto an isolated rod also generates an inward current that is associated with an increase of current fluctuations (Fig. 2 *A*). The single-channel current can be estimated from the variance-versus-mean current curve at low open probabilities:

$$\mathrm{Var}(I)/I = i(1 - p). \quad (4)$$

The single-channel current can thus be estimated from the limiting slope of the variance-versus-mean curve at small p. The single-channel current in rods is estimated to be 0.037 ± 0.0025 pA (n = 3) (Fig. 2 *B*), at a holding potential of −50 mV, indicating a single-channel conductance of 0.74 ± 0.05 pS (n = 3). The power spectrum of the current is best fitted to a Lorentzian with a corner frequency of 55 ± 5 Hz (n = 3) (Fig. 2 *C*). At this glutamate concentration, the open probability remains low, as seen by the linear variance-versus-mean curve. For $p \ll 1$, the opening rate is much smaller than the closing rate and the reciprocal of the corner frequency can therefore be considered in a first approximation to provide an estimate of the open lifetime for the channel. With this approximation, the mean open lifetime is estimated at 3 ms ± 0.25 ms (n = 3). These measurements indicate that the glutamate-activated channels in rods are similar to the ones characterized in cones.

D,L-Threo-3-hydroxyaspartate: a partial agonist

In cones, D,L-threo-3-hydroxyaspartate (THA), a substrate of glutamate transporters (Barbour et al., 1991), elicits an inward current that is also associated with an increase in current fluctuations (Fig. 4 *A*). However, the current with a saturating THA concentration (2.5 mM) averaged only 28% ± 5% (n = 6) of the maximum current obtained with glutamate (1 mM). Saturating concentration for THA was considered to be 2.5 mM because 0.25 mM THA generated 92.5 ± 5% (n = 3) of the response obtained with 2.5 mM THA. To understand the origin of this decrease in the maximum current, we determined the channel characteristics with THA. For applications of up to 2.5 mM THA, the variance-versus-mean current curve is best fitted with a linear function. This observation indicates that the open probability of the channel remains small even in the presence of a saturating THA concentration. The single-channel conductance is estimated to be 0.61 pS ± 0.11 pS (n = 5) (Fig. 4 *B*). The reduction of the saturating current therefore results from a decrease in the open probability of the channel rather than a decrease in its single-channel conductance. Because the channel conductance remains unchanged with THA, the maximum open probability of the channel is decreased to the same extent as the maximum macroscopic current (28% of maximum). The maximum open probability

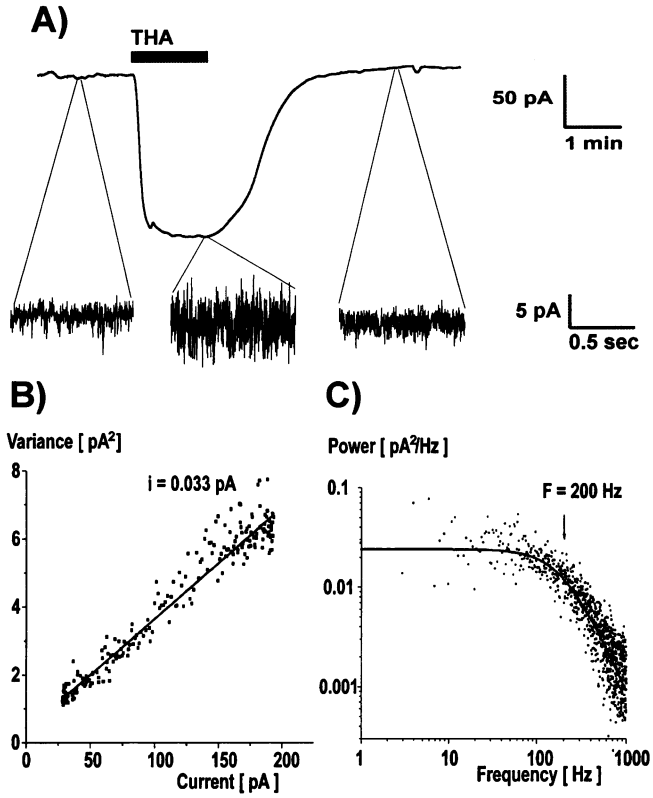

FIGURE 4 Characteristics of the channel with THA as the agonist. (*A*) A whole-cell recording from a cone photoreceptor held at −50 mV during a bath application of 0.5 mM THA. This increase of current was accompanied by a visible increase in noise. The signal is filtered at 1000 Hz. (*B*) Variance-versus-mean plot for a whole-cell current from a cone held at −50 mV during a washout of 0.5 mM THA. The best fit to a straight line is 0.033 pA. The single-channel conductance is 0.66 pS. (*C*) Power spectrum from a cone held at −50 mV during the application of 2.5 mM THA. The 1/*f* background noise has been numerically subtracted. The corner frequency of the Lorentzian is 200 Hz.

of the channel has therefore decreased from 0.7 with glutamate to 0.2 (= 28% of 0.7) with THA. It appears that THA is a partial agonist for the glutamate-activated channel, giving a lower maximum probability of opening at saturating concentrations.

The power spectrum of the THA-elicited current is also best fit to a single Lorentzian. The corner frequency has shifted to higher frequencies, 197 ± 3 Hz (n = 3) (Fig. 4 *C*) compared to the spectrum of the glutamate-elicited current at the same open probability (80 ± 10 Hz, n = 5). The higher corner frequency indicates that at an open probability, 0.2, the opening and closing rates of the channel are higher with THA than with glutamate. This means that THA application leads to a shorter open state lifetime for the channel. This is consistent with THA's action as a partial agonist for the glutamate-gated chloride channel.

Sodium dependence of the single-channel properties

The glutamate-elicited current exhibits an absolute dependence on external sodium. From the noise spectra, we can

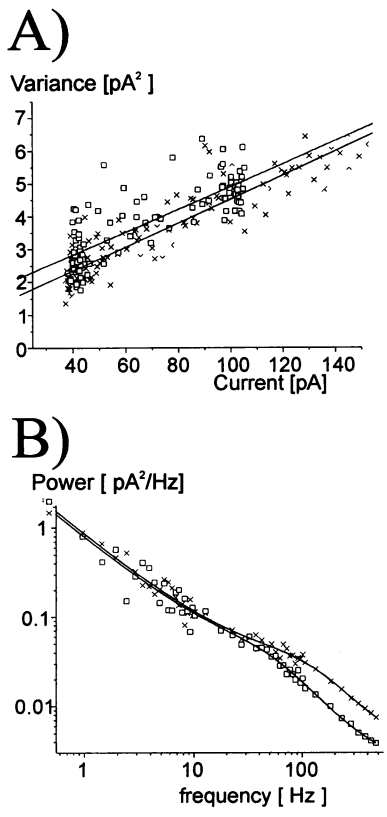

FIGURE 5 Sodium dependence of the glutamate-activated channel. (*A*) Variance-versus-mean plot of the currents of a cone with 12 mM sodium (90 mM lithium) (+) or 100 mM sodium (○) in the extracellular solution. The cell was held at −50 mV and the measurements were done on a washout of 37 μM free glutamate. The single-channel current is 0.036 pA and the single-channel conductance is 0.72 pS for both conditions. (*B*) Power spectra of the steady-state current from a cone at −50 mV during a 37 μM free glutamate application. Extracellular solution contained 90 mM lithium and 12 mM sodium (+), or 100 mM sodium (□). The background 1/*f* noise has not been subtracted but kept for comparison. The corner frequency of the Lorentzian is 59 Hz (+) in 12 mM sodium and 110 Hz ([□) in 100 mM sodium.

test whether sodium affects the channel conductance or its open probability. Decreasing the external sodium concentration from 100 to 12 mM in the extracellular solution decreased the macroscopic current to 42 ± 8% (n = 5). In 12 mM external sodium, the variance-to-mean ratio for the current was 0.037 ± 0.0025 pA (Fig. 5 *A*), indicating that the single-channel conductance remains unchanged at 0.74 ± 0.05 pS (n = 14; 13 cones, one rod) in low external sodium.

The power spectrum is shifted toward higher frequencies when the external sodium concentration is increased during a 37 μM free glutamate application. The corner frequency in 12 mM external sodium is 66 ± 10 Hz (n = 5), whereas it increases to 118 ± 10 Hz (n = 6) in 100 mM external sodium (Fig. 5 *B*).

These results show that external sodium affects the amplitude of the glutamate-elicited current by changing the probability of channel opening. Increasing the sodium concentration increases the open probability and increases the corner frequency in a manner parallel to that of glutamate. A parallel increase of the open probability and the corner frequency indicates that external sodium mainly affects the opening rate of the channel and thus external sodium appears to play the role of a co-agonist for the channel together with glutamate.

DISCUSSION

We showed that the glutamate-elicited chloride current is generated by as many as 20,000 channels with an estimated single-channel conductance of 0.7 pS and a maximum open probability of 0.7 in cones. The corner frequency increased from 80 to 215 Hz for free glutamate concentrations from 6 μM to 1 mM. External sodium appeared to play the role of a co-agonist of the ligand-gated channel with glutamate. THA, a glutamate transport blocker, was shown to be a partial agonist of the glutamate-gated channel. These results obtained about the glutamate-gated chloride channel from cones may also apply to rod photoreceptors, as we found that the glutamate-elicited current in rods is generated by a channel with the same single-channel conductance and a similar corner frequency at low open probability. These biophysical results are all consistent with glutamate gating of a chloride channel with an unusual sodium dependence and pharmacology.

In this analysis, we have assumed that the underlying unitary current is carried by chloride ions. Earlier work on the macroscopic glutamate-induced current showed that the reversal potential follows E_{Cl}, the Nerst potential for chloride (Sarantis et al., 1988; Picaud et al., 1995a). How sure can we be that the glutamate-induced noise emanates from the same process that produces the macroscopic chloride current? In the noise experiments, the fit of the variance-versus-mean plot to a parabola symmetric about p = 1/2 can be regarded as evidence that the noise and the macroscopic current emanate from a unique dose-response relation for glutamate. Furthermore, the fact that the noise and the macroscopic current scale linearly for different sodium concentrations and THA applications, and at different voltages, makes it highly unlikely that the noise is produced by a current other than the chloride current identified in the earlier work.

Model of a glutamate transporter with a chloride channel

The results of the noise analysis showed that the chloride channel behaves like a sodium/glutamate-gated chloride channel. The gating of the channel is controlled by the same conditions that control the glutamate uptake mechanism, i.e., they share the same pharmacology (Tachibana and Kaneko, 1988; Eliasof and Werblin, 1993) and ionic requirements (Picaud et al., 1995a). A simple model that

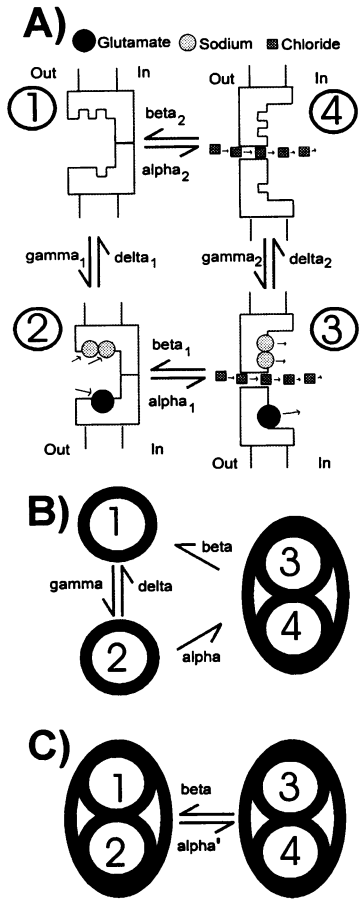

FIGURE 6 Sodium/glutamate cotransporter with a chloride channel. (*A*) A four-state model of a sodium/glutamate transporter that harbors a chloride channel: 1) A sodium and a glutamate binding site are exposed to the external surface. In this conformation the chloride channel is closed. 2) Sodium and glutamate bind to their binding sites. 3) The binding of sodium and glutamate induces a conformational change that exposes the sodium and glutamate sites to the internal surface. In this conformation the chloride channel is open. 4) The sodium and glutamate ions dissociate. The empty carrier returns to the resting state. (*B*) The three-state approximation in uptake mode. The approximation is made under the assumptions that the closing rate of the channel with ligand bound (β_1) is slow, the closing rate of the channel without ligand (β_2) is fast, and the concentration of ligands inside the cell is low, i.e., the association rate γ_2 is slow. (*C*) The two-state approximation in uptake mode. At infinite external ligand concentration the three-state model reduces to this two-state model where then the opening rate α' is equal to α.

would explain both the channel characteristics and the transporter pharmacology of the current is a glutamate transporter that harbors a chloride channel (Fig. 6 *A*). Although we cannot rule out the possibility that the chloride current is generated by a sodium/glutamate-gated channel unrelated to the sodium/glutamate transporter, the model will be seen to explain the correlations between transporter and channel functions.

The model is also supported by the recent cloning of several brain sodium/glutamate transporters that exhibit a chloride conductance when expressed in oocytes (Wadiche et al., 1995; Fairman et al., 1995). Such a hybrid transporter would transport glutamate in a sodium/potassium-dependent manner and simultaneously conduct chloride via a pore whose gating is keyed to the conformation change of the transporter. In this paper for simplicity we only consider the sodium and glutamate dependency of the transporter/channel, even though it has also been shown to have a potassium dependency (Picaud et al., 1995a). The transporter would have four states. There are two states (ligands bound and ligands unbound) with the binding sites for glutamate and sodium exposed to the external surface. In these two states the chloride channel is closed. In the two other states, ligands bound and ligands unbound with the binding sites exposed to the internal surface, the chloride channel is open. The binding of the ligands stabilizes the open conformation as it does for a ligand-gated channel. The chloride flux and the sodium/glutamate transport appear in Fig. 6 *A* to go through the same pore. The figure could also have been drawn with two separate pathways, one for the chloride flux and one for the sodium/glutamate transport, but with strict coupling of the conformational change in the transport pore to the gating of the chloride channel.

A feature of this transport/channel hybrid model is that internal ions should have an effect on the gating of the chloride channel. It has been shown that internal ions do change the magnitude and the voltage dependence of the chloride current, most likely by changing the gating of the channel (Picaud et al., 1995a). This is a feature that is not seen with conventional ligand-activated channels but could be explained by binding of ligands to the internal side of the transporter/channel hybrid, which would alter the open and closed lifetimes of the channel. The open probability of the four-state sodium/glutamate transporter/chloride channel model depends, hence, on the ligand concentrations on both sides of the membrane.

During a ligand-activated conformation change, this model of a transport protein would transport one glutamate and two sodiums per opening of the channel. From the noise experiments we know that the channel is open on average for 2 ms and thus lets through 500 chloride ions per opening, so the main current would be the chloride flux. The glutamate-induced current recorded in chloride-free solutions can probably serve as an estimate of the actual glutamate/sodium transport current, because the glutamate transport rate was shown to be independent of the chloride concentrations for the cloned glutamate transporters (Wadiche et al., 1995; Fairman et al., 1995). Recordings from cone photoreceptors in chloride-free solutions gave a glutamate-activated macroscopic current of only a few picoamperes (Picaud et al., 1995a). The contribution of the glutamate/sodium transport flux to the macroscopic current recorded in chloride solutions would hence be negligible. Thus, the reversal potential, the single-channel conductance, and the current noise would all be those of the chloride channel. But the gating of the channel would be under the same control as the glutamate

uptake and would hence display the same pharmacology and ionic requirements as the glutamate uptake mechanism. This model reconciles the two different mechanisms, a glutamate transporter or a glutamate-activated chloride channel, proposed for the generation of the glutamate-elicited current in photoreceptors.

Similarities with a ligand-activated channel

The resemblance of the transport/channel model to a ligand-gated channel is more obvious for a simplified three-state version of the transporter/channel. In the kinetic conditions that prevail in our noise experiments, the uptake cycle of the four-state transporter model can be approximated by a three-state model cycling counterclockwise (Fig. 6 *B*). The principal assumption made for this approximation is that the liganded protein is more stable in the open conformation and that the unliganded protein is more stable in the closed conformation. Furthermore, the association rate from the internal side can be neglected when the concentration of ligand is very low inside the cell. This model has properties very similar to those of a three-state ligand-activated channel. The different rate constants in the three-state model and their dependence on the different ligands can now be estimated from the results of the noise analysis.

Rate constants calculated from the power spectra

In the three-state approximation, the rate constants α, β, δ are independent of the external ligand concentration, in contrast to γ. Both α and β can be obtained at infinite ligand concentration when the model becomes equivalent to a two-state model with closing rate β and opening rate α (Fig. 6 *C*).

In this two-state approximation, the corner frequency of the power spectrum and the probability of opening are both related to the opening (α) and closing (β) rates of the channel.

$$f_{\text{corner}} = (\alpha + \beta)/2\pi \quad (5)$$

$$p = \alpha/(\alpha + \beta) \quad (6)$$

At saturating concentration, the power spectrum is best fit with a Lorentzian having a corner frequency of 220 Hz, and from the variance versus mean we get the maximum open probability of 0.7. Using these measurements of both the open probability p and the corner frequency, α and β were calculated from Eqs. 5 and 6. α and β were estimated at 967 s^{-1} and 415 s^{-1}, respectively. This gives an open lifetime for the channel ($1/\beta$) of 2.4 ms and a closed lifetime ($1/\alpha$) of 1.1 ms at saturating glutamate concentration. The two other rates, γ and δ, can be estimated from the measurement of the corner frequency and the open probability at a nonsaturating glutamate concentration. At a concentration of 6 μM free glutamate, the power spectrum has a corner frequency of 80 Hz and an open probability $p = 0.2$. With these values one can calculate the two remaining rates in the three-state model (see Appendix). The estimate of δ is 17,300 s^{-1}. If one assumes that only one glutamate molecule is required to open the channel, then $\gamma = C \cdot [\text{glu}]$, where C is found to be $3.72 \cdot 10^8$ $s^{-1}mol^{-1}$. The value of p and the corner frequency can now be estimated for any glutamate concentration: for 37 μM free glutamate the open probability is predicted to be 0.50 and the corner frequency is 134 Hz. These are in close agreement to the measured values of 0.5 and 118 Hz. Fig. 7 shows the experimentally measured corner frequency as a function of the open probability. The solid line shows the predicted corner frequencies for the model.

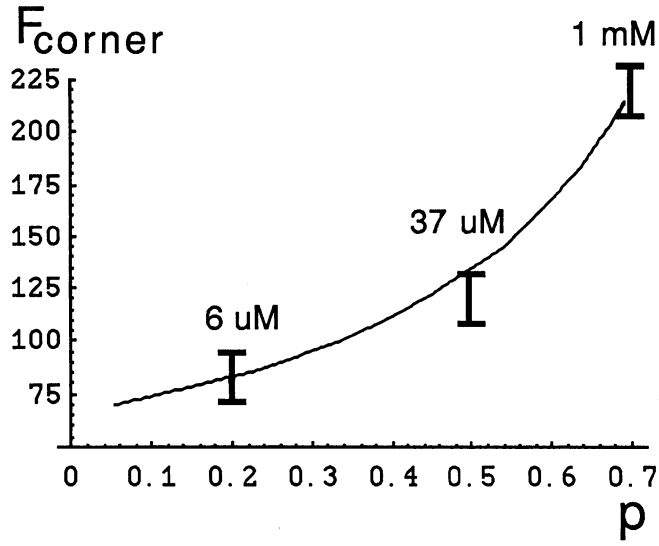

FIGURE 7 Corner frequency as a function of open probability. Corner frequency and open probability for 6, 37, and 1000 μM free glutmate. The solid line is the predicted lower corner frequency as a function of open probability for the three-state model found from Eqs. A1 and A4 in the Appendix.

The power spectrum of a three-state model should be a sum of two Lorentzians (Colquhoun and Hawkes, 1977). However, all of the observed power spectra were best fit with a single Lorentzian. This results from a limitation of the whole-cell recording technique. The cell capacitance and series resistance allow only a certain bandwidth for the recordings, which might exclude the predicted second Lorentzian. The bandwidth of the recordings in this study never exceeded 1000 Hz, which would leave the predicted second Lorentzian outside the bandwidth for all glutamate concentrations. The amplitude of the second Lorentzian would also be very small for the rates calculated and is probably not observable even with a higher bandwidth (see Appendix). The predicted second Lorentzian does not contribute much to the variance, because the amplitude of the second Lorentzian is very small

compared to the first Lorentzian (see Appendix). Therefore, the estimated single-channel conductance does not need to be corrected for the limited bandwidth of the recording.

The effects of THA explained in a three-state model

THA is considered to be a glutamate transport blocker because it inhibits glutamate uptake in synaptosomes (Bridges et al., 1991) and brain slices (Balcar and Johnston, 1972). However, THA is also known to be a competitive substrate for the glutamate transporter, as it is transported but at a much slower rate than glutamate (Balcar and Johnston, 1972; Barbour et al., 1991). In both rods (Grant, 1992) and cones (Picaud et al., 1995b), application of THA also elicited a current. We have shown here that this current is carried by the glutamate-gated chloride channel and that THA is a partial agonist for this channel.

Changing the agonist to THA would change all of the rates in the three-state model. Using an open probability of 0.2 and a corner frequency of 197 Hz, the opening rate α and closing rate β can be estimated at 248 s^{-1} and 1002 s^{-1}, respectively. An estimate for the open and closed lifetimes of the channel was therefore 1 ms and 4 ms, respectively, with a saturating THA concentration, in contrast to the 2.4-ms open and 1-ms closed lifetime for saturating glutamate concentration. It can be concluded that THA elicits a much smaller maximum response than glutamate because it opens the channel less often and for a shorter time than the endogenous agonist glutamate. Such properties of partial agonists have been reported with the single-channel recording technique for other glutamate receptors and ligand-gated channels (Jackson et al., 1982; Lecar et al., 1982; Cull-Candy and Parker, 1983). The blocking effect of THA on the glutamate-elicited current relies on the competitive binding of this partial agonist to the glutamate binding site.

The effects of sodium explained in a three-state model

Varying the sodium concentration did not alter the single-channel conductance or the mean open lifetime. However, increasing the sodium concentration increased the opening rate of the channel. Sodium appeared to play the role of a co-ligand, which is necessary for the channel to open. The simplest model that could incorporate the requirement that both sodium and glutamate have to bind to open the channel is the earlier three-state model with γ also dependent on the external sodium concentration: $\gamma = C^*[glu]_0^*([Na]_0)$. (The sodium dependence of the glutamate-activated current was found to be fit with a Hill coefficient of $n = 1.5$ (Picaud et al., 1995a). Here we have used $n = 1$ for the sodium dependency.) This will give C a value of $3.72 \cdot 10^9$ $s^{-1}mol^{-2}$ because γ was evaluated for 100 mM sodium and a free glutamate concentration of 37 μM.

The other rate constants would all be independent of external sodium and glutamate concentrations. The predicted open probability and corner frequency for 12 mM sodium and 37 μM free glutamate are 0.16 and 79 Hz (see Appendix). These values are similar to the observed open probability of 0.2 and the observed corner frequency of 66 Hz.

CONCLUSIONS AND PREDICTIONS

This model of a transporter/channel hybrid reconciles the two different mechanisms, chloride channel and glutamate transporter, that have been proposed to generate the glutamate-elicited current in photoreceptors. The model also gives some predictions about the glutamate-uptake rates. The maximum rate of uptake $(1/\alpha + 1/\beta)^{-1}$ for this model would be 290 s^{-1} for glutamate and 200 s^{-1} for THA. This hypothesized slower rate for the maximal THA transport, 70% of the maximal glutamate transport, has been observed for the cloned glutamate transporter GLAST-1 when expressed in oocytes (Klockner et al., 1994).

The transporter/channel model is able to explain the different effects of external glutamate, sodium, and THA on the chloride current shown in this paper. Both the macroscopic currents and the single-channel kinetics are well described by this model of a transporter with a chloride-channel leak.

APPENDIX: THEORY OF THE POWER SPECTRUM

Here we show that the transition rates in the model can be determined from the lower corner frequency of the power spectrum and the open probability of the channel. We also show that the measured single channel conductance from the variance-versus-mean curve is an accurate estimate in these limited bandwidth recordings for these rates.

For our experimental conditions the four-state model (Fig. 6 *A*) can be approximated with a three-state model (Fig. 6 *B*). The two models would display the same basic noise characteristic in these limited-bandwith recordings. They can both be approximated with a pseudo two-state model of an ion channel with an opening rate $\alpha' = \alpha/(1 + (\delta + \alpha)/\gamma)$ and a closing rate β (Fig. 6 *C*). The four rate constants in the three-state model can all be determined from the noise analysis data. Similarly, the four corresponding rates in the four-state model can be determined under the assumptions made for the other rates ($\alpha_2 \ll \alpha_1$, $\gamma_2 \ll \delta_2$, and $\beta_2 \gg \delta_2 \gg \beta_1$). The closing rate β in the three-state model is, under these assumptions, approximately equal to the dissociaton rate δ_2 in the four-state model.

At steady state, the open probability p_{open} for the three-state approximation is equal to

$$\bar{p}_{open} = \frac{1}{1 + \frac{\beta}{\alpha}\left(1 + \frac{\delta + \alpha}{\gamma}\right)}. \qquad \text{(A1)}$$

($p_{open} \equiv$ probability of the channel being in the open state, i.e., the collapsed states 3 and 4 in Fig. 6 *B*).

The average macroscopic current from N channels with a single-channel current i and three states like the model in Fig. 6 B is

$$I(t) = Nip_{open}(t) \tag{A2}$$

$$p_{open}(t) = \bar{p}_{open} + Ae^{-\lambda_1 t} + Be^{-\lambda_2 t}, \tag{A3}$$

where λ_i is found as the solution to the equation

$$\lambda^2 - (\alpha + \beta + \delta + \gamma)\lambda + (\alpha\gamma + \beta\delta + \gamma\beta + \alpha\beta) = 0$$

$$\lambda_{1,2} = \frac{\alpha + \beta + \delta + \gamma}{2} + \sqrt{\frac{(\alpha + \beta + \delta + \gamma)^2}{4} - (\alpha\gamma + \beta\delta + \gamma\beta + \alpha\beta)}. \tag{A4}$$

The power spectrum of the current I from a three-state model is a sum of two Lorentzians with corner frequencies $f_i = \lambda_i/2\pi$ (Colquhoun and Hawkes, 1983).

Application of infinite glutamate concentration reduces the three-state model to a two-state model, where α and β can be determined from the observed open probability and the corner frequency. The two rate constants were found to be $\alpha = 967\ s^{-1}$ and $\beta = 415\ s^{-1}$ (see Discussion).

We can then determine the two remaining rate constants δ and γ by using the open probability and lower corner frequency found for a different glutamate concentration and solving Eqs. A1 and A4 for γ and δ. For a 6 μM glutamate application the observed corner frequency is 80 Hz and the open probability is 0.21. This gives a $\delta = 17{,}320\ s^{-1}$ and $\gamma = C' \cdot$ [glutamate], with $C' = 3.72 \cdot 10^8\ s^{-1}mol^{-1}$.

The open probability and the corner frequencies can now be estimated for any glutamate concentration from Eqs. A1 and A4. Furthermore, the effect of sodium on these observations can be predicted if one assumes that γ is also dependent on sodium, i.e., $\gamma = C$ [glu][Na]. The value of C is found to be $3.72 \cdot 10^9\ s^{-1}mol^{-2}$.

The second Lorentzian is predicted, for all glutamate concentrations, to lie outside the bandwidth of the recording (<1 kHz). Because the single-channel conductance is estimated from the variance, which is proportional to the integral of the whole power spectrum, we have to estimate how much of the variance is in this second Lorentzian.

The power spectrum $W(f)$ is the Fourier transform of the autocorrelation function $C(t)$ (Wiener-Kintchine theorem):

$$W(f) = 4\int_0^\infty C(t)\cos(2\pi ft)dt. \tag{A5}$$

The autocorrelation function $C(t)$ for the three-state model is

$$C(t) = N^2i^2\langle(p_{open}(0) - \bar{p}_{open})(p_{open}(t) - \bar{p}_{open})\rangle, \tag{A6}$$

Where $\langle\ \rangle$ is the average over all possible initial states.
By using the initial condition $\Delta p_i(0) \equiv (p_i(0) - p_i)$ one can find the values of A and B that are necessary to calculate the autocorrelation function (p_i = the probability of finding the channel in state i):

$$\begin{aligned} \Delta p_{open}(0) &= p_{open}(0) - \bar{p}_{open} = A + B \\ \dot{p}_{open}(0) &= \alpha p_2(0) - \beta p_{open}(0) = -\lambda_1 A - \lambda_2 B \end{aligned} \tag{A7}$$

Because

$$\beta\bar{p}_{open} - \alpha\bar{p}_2 = 0, \tag{A8}$$

this can be added to the left side of the second equation

$$\begin{aligned} \Delta p_{open}(0) &= A + B \\ \alpha\Delta p_2(0) - \beta\Delta p_{open}(0) &= -\lambda_1 A - \lambda_2 B \Rightarrow \end{aligned} \tag{A9}$$

This gives A and B as functions of $\Delta p_i(0)$:

$$\begin{aligned} A &= \frac{-\alpha\Delta p_2(0) + (\beta - \lambda_2)\Delta p_{open}(0)}{\lambda_1 - \lambda_2} \\ B &= \frac{-(\beta - \lambda_1)\Delta p_{open}(0) + \alpha\Delta p_2(0)}{\lambda_1 - \lambda_2} \end{aligned} . \tag{A10}$$

So the autocorrelation function $C(t)$ is

$$C\,t) = \frac{(\beta - \lambda_2)\langle\Delta p_{open}(0)^2\rangle - \alpha\langle\Delta p_{open}(0)\Delta p_2(0)\rangle}{\lambda_1 - \lambda_2}e^{-\lambda 1t} + \frac{\alpha\langle\Delta p_{open}(0)\Delta p_2(0)\rangle - (\beta - \lambda_1)\langle\Delta p_{open}(0)^2\rangle}{\lambda_1 - \lambda_2}e^{-\lambda_2 t}. \tag{A11}$$

There are three possible initial states for the channel:

I. Channel in state 1: $\{p_1^{I}(0) = 1;\ p_2^{I}(0) = 0;\ p_{open}^{I}(0) = 0\}$

II. Channel in state 2: $\{p_1^{II}(0) = 0;\ p_2^{II}(0) = 1;\ p_{open}^{II}(0) = 0\}$

III. Channel in the open state: $\{p_1^{III}(0) = 0;\ p_2^{III}(0) = 0;\ p_{open}^{III}(0) = 1\}$

State I occurs with probability p_1, state II occurs with probability p_2, and state III occurs with probability p_{open}. The ensemble averaging $\langle f(t)\rangle$ for a function $f(t)$ is equal to the sum of the value of $f(t)$ for each initial state weighted by the equilibrium probability for that initial state:

$$\langle f(t)\rangle = \sum_{i=I}^{III} \bar{p}_i f(t;p_0^i(0),p_1^i(0),p_2^i(0)). \tag{A13}$$

The averaging over all possible initial states gives

$$\begin{aligned} \langle(\Delta p_{open}(0)^2\rangle &= \bar{p}_{open}(1 - \bar{p}_{open}) \\ \langle\Delta p_{open}(0)\Delta p_2(0)\rangle &= -\bar{p}_{open}\bar{p}_2 + \langle p_{open}(0)p_2(0)\rangle \\ &= -\frac{\beta}{\alpha}\bar{p}_{open}^2 + \langle p_{open}(0)p_2(0)\rangle. \end{aligned} \tag{A14}$$

The last term on the right is equal to zero because the channel cannot be in two states at $t = 0$.

This gives $C(t)$ as

$$C(t) = \frac{\beta\bar{p}_{open} - \lambda_2\bar{p}_{open}(1 - \bar{p}_{open})}{\lambda_1 - \lambda_2}e^{-\lambda_1 t} + \frac{\beta\bar{p}_{open} - \lambda_1\bar{p}_{open}(1 - \bar{p}_{open})}{\lambda_2 - \lambda_1}e^{-\lambda_2 t}. \tag{A15}$$

So for the three-state model the power spectrum is a two-Lorentzian function given by

$$W(f) = 4\left(\frac{\beta\bar{p}_{open} - \lambda_2\bar{p}_{open}(1-\bar{p}_{open})}{(\lambda_1-\lambda_2)\lambda_1}\frac{1}{1+\left(\frac{2\pi f}{\lambda_1}\right)^2}\right. \quad \text{(A16)}$$
$$\left. + \frac{\beta\bar{p}_{open} - \lambda_1\bar{p}_{open}(1-\bar{p}_{open})}{(\lambda_2-\lambda_1)\lambda_2}\frac{1}{1+\left(\frac{2\pi f}{\lambda_2}\right)^2}\right).$$

The variance is the integral of the power spectrum:

$$\mathrm{var}(I) = \int_0^\infty W(f)\mathrm{d}f. \quad \text{(A17)}$$

The variance for the three-state model can be divided into two parts, $\mathrm{var}(I) = \mathrm{var}_1(I) + \mathrm{var}_2(I)$. Var_1 is the contribution from the first Lorentzian and var_2 is the contribution from the second Lorentzian. The ratio of the two contributions is

$$\frac{\mathrm{var}_2(I)}{\mathrm{var}_1(I)} = \frac{\lambda_1(1-\bar{p}_{open})-\beta}{\beta-\lambda_2(1-\bar{p}_{open})}. \quad \text{(A18)}$$

This ratio is <0.01 for all glutamate concentrations. A part of the second Lorentzian lies outside the bandwidth of the recording, and the variance from this part of the spectrum is thus not included in the variance measurement. But the amount of power in the second Lorentzian is very small compared to the first Lorentzian and hence the second Lorentzian would not contribute much to the variance. The estimate of the single-channel conductance can therefore be assumed to be an accurate estimation of the true single-channel conductance.

This work was supported by a Wenner-Gren fellowship to HPL; by HFSPO, NATO, Fondation Signer-Polignac and Fondation Philippe fellowships to SAP; by National Institutes of Health grant EY00561 to FSW; and by NSF grant 8904462 to HPL and HL.

REFERENCES

Balcar, V. J., and G. A. R. Johnston. 1972. The structural specificity of the high affinity uptake of L-glutamate and L-aspartate by rat brain slices. *J. Neurochem.* 19:2657–2666.

Barbour, B., H. Brew, and D. Attwell. 1991. Electrogenic uptake of glutamate and aspartate cells into glial cells isolated from the salamander (*ambystoma*) retina. *J. Physiol. (Lond.).* 436:169–193.

Bridges, R. J., M. S. Stanley, M. W. Anderson, C. W. Cotman, and A. R. Chamberlain. 1991. Conformationally defined neurotransmitter analogues. Selective inhibition of glutamate uptake by one pyrrolidine-2,4-dicarboxylate diastereomer. *J. Med. Chem.* 34:717–725.

Colquhoun, D., and A. G. Hawkes. 1977. Relaxation and fluctuations of membrane currents that flow through drug-operated channels. *Proc. R. Soc. Lond. B.* 199:231–262.

Colquhoun, D., and A. G. Hawkes. 1983. The principles of the stochastic interpretation of ion-channel mechanisms. *In* Single-Channel Recording, B. Sakmann and E. Neher, editors. Plenum Press, New York. 135–175.

Cull-Candy, S. G., and I. Parker. 1983. Experimental approaches used to examine single glutamate-receptor ion channels in locust muscle fibers. *In* Single-Channel Recording. B. Sakmann and E. Neher, editors. Plenum Press, New York. 389–400.

Eliasof, S., and F. S. Werblin. 1993. Characterization of the glutamate transporter in retinal cones of the tiger salamander. *J. Neurosci.* 13: 402–411.

Everett, K., M. Sarantis, and D. Attwell. 1990. A presynaptic action of glutamate on cone photoreceptors. *In* Sensory Transduction. A. Borsellino, L. Cervetto, and V. Torre, editors. Plenum Press, New York and London. 235–245.

Fairman, W. A., R. J. Vanderberg, J. L. Arriza, M. P. Kavanaugh, and S. G. Amara. 1995. An excitatory amino-acid transporter with properties of a ligand-gated chloride channel. *Nature.* 375:599–603.

Grant, G. B. 1992. Characterization and function of the electrogenic glutamate transporter in rod photoreceptors of the tiger salamander retina. PhD dissertation. University of California, Berkeley.

Grant, G. B., S. Eliasof, and F. S. Werblin. 1992. Sodium glutamate cotransporter in rod terminals is essential for rod input to horizontal cells of the tiger salamander. *Invest. Ophthalmol. Vis. Sci.* 33:1327.

Hammill, O. P., A. Marty, E. Neher, B. Sakmann, and F. J. Sigworth. 1981. Improved patch-clamp techniques for high-resolution current recording from cells and cell-free membrane patches. *Pflügers Arch.* 391:85–100.

Jackson, M. B., H. Lecar, D. A. Mathers, and J. L. Barker. 1982. Single channel currents activated by gamma-aminobutyric acid, muscimol, and (−)-pentobarbital in cultured mouse spinal neurons. *J. Neurosci.* 2:889–894.

Klockner, U., T. Storck, M. Conradt, and W. Stoffel. 1994. Functional properties and substrate specificity of the cloned L-glutamate/L-aspartate transporter GLAST-1 from rat brain expressed in *Xenopus oocytes. J. Neurosci.* 14:5759–5765.

Lecar, H., C. Morris, and B. Wong. 1982. Single-channel currents and the kinetics of agonist-induced gating. *In* Structure and Function of Excitable Cells. D. C. Chang, I. Tasaki, W. J. Adelman, Jr., and H. R. Leuchtag, editors. Plenum Publishing, New York. 159–173.

Marc, R. E., and D. M. K. Lam. 1981. Uptake of aspartic and glutamic acid by photoreceptors in goldfish retina. *Proc. Natl. Acad. Sci. USA.* 78: 7185–7189.

Martell, A. E., and R. M. Smith. 1974. *In* Critical Stability Constants, Vol. 1, Amino Acids. Plenum Press, New York. 27–28.

Picaud, S. A., H. P. Larsson, G. B. Grant, H. Lecar, and F. S. Werblin. 1995a. A glutamate-gated chloride channel with glutamate transport-Like properties in cone photoreceptors of the tiger salamander. *J. Neurophys.* 74:1760–1771.

Picaud, S. A., H. P. Larsson, D. P. Wellis, H. Lecar, and F. S. Werblin. 1995b. Cone photoreceptors respond to their own glutamate release in the tiger salamander. *Proc. Natl. Acad. Sci. USA.* 92:9417–9421.

Sarantis, M., K. Everett, and D. Attwell. 1988. A presynaptic action of glutamate at the cone output synapse. *Nature.* 332:451–453.

Tachibana, M., and A. Kaneko. 1988. L-Glutamate-induced depolarization in solitary photoreceptors: a process that may contribute to the interaction between photoreceptors in situ. *Proc. Natl. Acad. Sci. USA.* 85: 5315–5319.

Wadiche, J. I., R. J. Wanderberg, J. L. Arriza, S. G. Amara, and M. P. Kavanaugh. 1995. Ligand-gated chloride conductance associated with a human glutmate transporter. *Biophys. J.* 68:A437.